Melt electrowriting of amorphous solid dispersions: influence of drug and plasticizer on rheology and printing performance

Larissa Keßler[1], Robert Luxenhofer[1*]

[1]Soft Matter Chemistry, Department of Chemistry, and Helsinki Institute of Sustainability Science, Faculty of Science, University of Helsinki, PB55, 00014 Helsinki, Finland

Correspondence to:
Prof. Dr. R. Luxenhofer: robert.luxenhofer@helsinki.fi

Keywords

poly(2-oxazoline), poly(2-oxazine), indomethacin, amphiphilic block copolymers, plasticized polymer blends, sublingual drug delivery

Abstract

Drug loaded microfiber scaffolds have potential for sublingual drug delivery due to their fast dissolution time and tunable porosity. Such microfiber scaffolds can be prepared by melt electrowriting (MEW), wherein a polymer melt is electrostatically drawn out of a syringe onto a computer controlled moving collector. The fabrication of such scaffolds via MEW has previously been shown for a polymer with a glass transition temperature (T_g) just above room temperature, making handling challenging. For this reason, ABA triblock copolymers bearing poly(2-oxazoline) and poly(2-oxazine) with slightly higher T_g were synthesized and their processability into drug loaded microfiber scaffolds was assessed. Additionally, plasticizers commonly used in drug products were added to decrease the fabrication temperature. The aim was to investigate the influence of plasticizers on the melt viscosity and printability to expand the polymer platform for the preparation of drug loaded microfiber scaffolds.

Temperature dependent melt rheology measurements of the polymers and their mixtures revealed a drop in viscosity by one order of magnitude by the addition of triethyl citrate and ethylene glycol, respectively. Addition of the model drug indomethacin led to a further decrease in viscosity. Even though the drug loaded samples were printable with and without the addition of triethyl citrate, better fiber stacking and therefore improved printing results were obtained with the plasticizer added. However, the addition of the plasticizer did alter the dissolution profile for some of the polymer samples, leading to longer dissolution times or lower drug release compared to the samples without plasticizer, which makes it difficult to predict the influence of the plasticizer on the dissolution profile.

1 Introduction

Taking large pills can be problematic for patients with swallowing difficulties, the elderly and children.[1] One way to overcome this challenge is the use of sublingual or buccal application forms. Due to the high number of capillaries in the mouth floor and the relatively permeable mucosa, the drug can be taken-up rapidly by the body.[2] This allows the drug to enter the blood flow without the influence of the intestine, gastric acid and first pass effect.[3] Additionally, this can lead to a shorter onset time to reach the minimal effective concentration with lower drug doses compared to oral administration.[4]

Another challenge is the poor water solubility of new drugs and drug candidates.[5] One method to increase the apparent water solubility of the drug is the preparation of the amorphous form of the drug, as this can improve the dissolution rate and oral bioavailability. However, the physical instability and recrystallization tendency of the amorphous form is a major issue. To overcome this, amorphous solid dispersions (ASDs) can be prepared, wherein the amorphous form of a drug is stabilized using suitable excipients, e. g., through tuning the interactions between polymeric excipients and drugs.[6-9] This is not only stabilizing the amorphous form, but also influencing the dissolution profile and therefore the bioavailability of the drug.[10] Common polymer excipients for the preparation of ASDs are poly(vinyl pyrrolidone)[11], poly(vinyl pyrrolidone-co-vinyl acetate)[12] or hydroxypropyl methylcellulose[13-14]. Previously, poly(2-oxazoline) (POx) and poly(2-oxazine) (POzi) bearing polymers were explored as excipients.[15-17] Especially, amphiphilic ABA triblock copolymers comprising POx/POzi have been used for the formulation of drugs with low water solubility with drug loading up to 50wt%.[18-24] More recently, these polymers were studied regarding the stabilization of drug nanocrystals[25] and in drug loaded microneedles[26].

A well-studied additive manufacturing (AM) method for the preparation of fiber mats with high surface area is solution electrospinning. With this method fibers mats with poorly controllable fiber placement, but low fiber diameter can be prepared.[27] However, usually the use of (toxic) solvents is necessary. To avoid the use of solvents, melt electrospinning can be an alternative to produce fiber mats with poorly controllable fiber placement. With both techniques, drug loaded fiber mats were prepared with drug release varying form several minutes to month, depending on the polymer matrix and drug used.[28-33]

Another AM technique for the preparation of ASDs with high drug loading is melt electrowriting (MEW), which allows accurate microfiber placement on a computer controlled moving collector. The fiber diameters achieved by using this technique are usually ranging from 5 to ~50 µm with the possibility of producing unique and highly defined printing patterns. The printed fiber mats have a high surface area which can result in fast dissolution. Previously,

drug loaded scaffolds were prepared with drug release varying from minutes to several hours.[15, 34-35] The longer drug release was achieved by using poly(ε-caprolactone) as polymer matrix[34-35], whereas shorter drug release times with dissolution of the whole scaffold were observed by using an amphiphilic ABA triblock copolymer comprising poly(2-oxazine) (POzi) and poly(2-oxazoline) (POx).[15] Here, high drug loading and dissolution within 1 - 5 min depending on the drug loading was achieved. However, the due to the low glass transition temperature (T_g) of the polymer, the sample preparation needed additional hot melt extrusion for sufficient mixing of polymer and drug.

One drawback for the use of MEW is that typically high temperatures are needed to obtain a sufficiently low viscous polymer melt, which can be further processed. To lower the fabrication temperature, plasticizers can be used, which can improve the processability by reducing the polymer melt viscosity.[36] However, some requirements need to be met: low volatility, high temperature stability and good compatibility with the polymer.[37] If the plasticizer is used in an ASD, the influence of plasticizer on the dissolution rate of the drug if of interest.[38] Importantly, plasticizers was shown to influence the melt viscosity of different grades of poly(vinyl alcohol) to a different extend, which suggests the need for optimization for every polymer-plasticizer combination.[39] Previously used plasticizers are small molecules, like citrate derivates[39], mono-[40] and polysaccharides[41], glycerol[42] or PEG[43] based compounds or even small molecule drugs[44-45] or pharmaceutically active ionic liquids[46].

The aim of this work was to explore the influence of the plasticizer and drug on the viscosity on four amphiphilic ABA triblock copolymers to decrease the fabrication temperature necessary for melt electrowriting. In this study, melt viscosity and T_g values of the polymers, the polymer-drug mixtures and the polymer-drug-plasticizer mixtures were studied. Selected samples were used for MEW fabrication and evaluated regarding their printability and dissolution profile.

2 Materials and Methods

2.1 Chemicals

Indomethacin (IND) was purchased from TCI chemicals (Zwijndrecht, Belgium), 3-amino-propanol, 2-amino-ethanol, valeronitrile, hexaennitrile, 2-methyl-2-oxazoline, benzonitrile, calcium hydride, phosphorus pentoxide, methyl triflate, piperidine and zinc acetate dihydrate from Sigma-Aldrich (Helsinki, Finland). Dichloromethane, sodium sulfate, triethyl citrate, citric acid and triacetine were purchased from Fisher Scientific (Vantaa, Finland). All chemicals were used as received unless otherwise stated.

2-methyl-2-oxazoline was dried by stirring over CaH_2 under inert atmosphere, followed by distillation prior to use. Benzonitrile was dried by refluxing over P_2O_5 under inert atmosphere, followed by distillation prior to use.

2.2 Monomer Synthesis

The monomers 2-*n*-butyl-2-oxazoline (BuOx), 2-*n*-butyl-2-oxazine (BuOzi), 2-*n*-pentyl-2-oxazoline (PentOx) and 2-*n*-pentyl-2-oxazine (PentOzi) were synthesized following the procedure by Witte and Seeliger.[47] Briefly, for BuOx and BuOzi, in a nitrogen flushed flask valeronitrile (for PentOx and PentOzi hexanenitrile), 3-amino-propanol (for the 2-oxazine synthesis or 2-amino-ethanol for the 2-oxazoline synthesis) and catalytic amounts of zinc acetate dihydrate were mixed and heated to 130 °C and the progress was controlled by ^{1}H NMR spectroscopy. After completion of the reaction, the mixture was dissolved in dichloromethane and washed with H_2O three times. The organic layer was dried with Na_2SO_4 and concentrated. The raw product was dried with CaH_2 and distilled under reduced pressure under nitrogen atmosphere to yield the product as a colourless liquid. Detailed amounts can be found in the Supporting Information (Supporting Information Table S1 – S4, Figure S1 – S4).

2.3 Polymer Synthesis

The polymer synthesis and workup procedures were carried out as described elsewhere.[20] Details can be found in the Supporting Information (Supporting Information Table S5 – S8, Figure S5 – S8). Briefly, methyl triflate was added to a dried and nitrogen-flushed Schlenk flask and dissolved in the respective amount of benzonitrile. MeOx was added, and the reaction mixture was heated to 120 °C and stirred until ^{1}H NMR spectroscopy revealed complete consumption of the monomer. Subsequently, the mixture was cooled to room temperature and the monomer for the second block, 2-*n*-butyl-2-oxazine, 2-*n*-butyl-2-oxazoline, 2-*n*-pentyl-2-oxazoline and 2-*n*-pentyl-2-oxazine, respectively, was added. The mixture was heated to 130 °C overnight. For polymers containing PentOzi, the polymerization

was heated to 150 °C until complete consumption of the monomer for the second block. The same procedure (120 °C) was repeated for the third block MeOx. After confirmation of monomer consumption by ^{1}H NMR, the polymerization was terminated by addition of ethyl isonipecotate or piperidine at 50 °C for 4 h. The solvent was removed under reduced pressure. The polymer was transferred into a dialysis bag (MWCO 1 kDa, cellulose acetate, Spektrum™, Rancho Dominguez, CA, USA) and dialysed against deionized water for two days with several water changes. Afterwards, the solution was recovered from the bag and lyophilized.

2.4 Nuclear Magnetic resonance Spectroscopy (NMR)

^{1}H NMR spectra were measured with an Avance III 500 MHz spectrometer from Bruker Biospin (Ettlingen, Germany) at a temperature of 25 °C (298 K). The spectra were calibrated on the solvent signal of CD_2Cl_2 (5.32 ppm) or $CDCl_3$ (7.26 ppm).

2.5 Size Exclusion Chromatography (SEC)

SEC was measured with a Waters Acquity APC system, equipped with Acquity Column Manager – S, Sample Manager – pFTN, Isocratic Solvent Manager, Acquity RI Detector and Aquity TUV Detector (Waters Corporation, Milford, MA, USA). The used columns are Acquity APC XT 45, 125 and 200. The eluent was dimethylformamide (DMF, Fisher Scientific, Vantaa, Finland) with a flow of 0.6 mL/min and at a temperature of 40 °C. The system was calibrated with poly(methyl methacrylate) (PMMA) standards (Polymer Standard Service, Agilent, Espoo, Finland). The data were analysed using Empower 3 and OriginPro (OriginLab Corporation, Northampton, MA, USA).

2.6 Differential Scanning Calorimetry (DSC)

DSC was conducted using a DSC Q2000 (TA Instruments, Newcastle, DE, USA). Samples of about 10 mg were prepared in sealed aluminium pans and heated from +5 °C to +200 °C and subsequently cooled to −50 °C at a linear rate of 10 °C min^{-1} in a nitrogen atmosphere. This cycle was repeated three times, with a final cooling to room temperature. The glass transition temperature (T_g) was obtained from the inflection point of the second and third heating cycle and the melt temperature (T_m), if applicable, as the peak maximum of the endothermic curve in the first heating. The data were evaluated using Origin software.

2.7 Ultraviolet-Visible (UV-Vis) Spectroscopy

UV-Vis experiments were performed on a BioTek Synergy H1 plate reader (Agilent, Espoo, Finland) at a wavelength of 340 nm. A standard curve of IND was obtained by quantifying

known amounts (Supporting Information Figure S9). The data were analyzed using the Origin software.

2.8 Preparation of polymer blends

For the preparation of the polymer blends used in MEW printing, DSC analysis and melt viscosity measurements, the different components were weighted and physically blend for 10 min using a mortar and pestle until a homogenous blend was obtained. The detailed equivalents for the different blends can be found in Table 1.

Table 1. Equivalents of polymer, drug and plasticizer used for the polymer–drug-plasticizer blends.

	polymer [eq.]	IND [eq.]	plasticizer [eq.]
polymer + plasticizer	1	n.a.	0.05
polymer + IND	1	1	n.a.
polymer + plasticizer + IND	1	1	0.05

2.9 MEW printing

A custom-built MEW printer similar to a previously described machine[48] was used to process the polymer plasticizer-blends, polymer-drug blends and polymer-plasticizer-drug blends. The 3 mL glass syringes (Poulten & Graf GmbH, Wertheim, Germany) were loaded with different materials and heated for a minimum of 30 minutes prior to printing until the bubbles within the melt dissipated. For all experiments, a nozzle tip with an inner diameter of 0.65 mm (23G) was used and manually grinded to a length of 13 mm. Other applied printing parameters are listed in Table 2 and Table 3.

Table 2. MEW printing parameters for the polymers-plasticizer blends with triethyl citrate (TEC), triacetin or ethylene glycol as plasticizers.

	NT^a [°C]	ST^b [°C]	TS^c [mm/min]	V^d [kV]	p^e [bar]	T_c^f [°C]	FD^g [µm]	FS^h [mm]
A-PentOx-A	155	155	540	5.2	1	24	55 ± 11	1.29 ± 0.06
+ TEC	160	160	600	4.3	1	25	46 ± 7	1.31 ± 0.05
	165	165	780	4.2	1	27	47 ± 11	1.34 ± 0.1
A-PentOx-A	155	155	480	5.2	1	27	77 ± 14	n.a.
+ triacetin	160	160	300	5.1	1	27	65 ± 10	n.a.
A-PentOx-A	155	155	480	4.9	1.1	28	78 ± 6	n.a.

+ ethylene	160	160	480	5.4	1	28	58 ± 5	1.29 ± 0.07
glycol	165	165	660	5.4	1	29	46 ± 6	1.33 ± 0.08
A-BuOzi-A +	155	155	360	4.1	1	25	75 ± 8	n.a.
TEC	160	160	420	5	1	25	68 ± 10	1.22 ±0.09
	165	165	420	6.5	1	26	46 ± 8	1.24 ± 0.06
A-BuOzi-A	155	155	360	6.2	1	27	45 ± 9	n.a.
+ ethylene	160	160	480	5.9	1	27	65 ± 8	1.35 ± 0.1
glycol	165	165	600	3.6	1	28	71 ± 18	1.24 ± 0.1
A-BuOx-A	160	160	240	5.8	1	25	72 ± 10	1.35 ± 0.07
+ ethylene	165	165	240	5.5	1	26	67 ± 13	1.37 ± 0.05
glycol	170	170	480	5.2	1	27	61 ± 11	1.39 ± 0.07
A-PentOzi-A	160	160	180	6.0	1	25	61 ± 10	n.a.
+ TEC	165	165	180	4.3	1	25	59 ± 10	n.a.
	170	170	180	4.5	1	25	66 ± 7	1.37 ± 0.09
A-PentOzi-A	160	160	180	4.8	1	27	47 ± 8	n.a.
+ ethylene	165	165	180	5.5	1	28	53 ± 7	n.a.
glycol	170	170	180	5.5	1	29	43 ± 7	1.46 ± 0.04

[a] nozzle temperature; [b] syringe temperature; [c] translation speed; [d] applied voltage; [e] applied pressure; [f] collector temperature; [g] fiber diameter; [h] fiber spacing.

Table 3. MEW printing parameters for samples containing the IND loaded polymer blends with and without the plasticizer triethyl citrate (TEC).

	NT[a] [°C]	ST[b] [°C]	TS[c] [mm/min]	V[d] [kV]	p[e] [bar]	T_c[f] [°C]	FD[g] [µm]	FS[h] [mm]
A-PentOx-A +IND	125	125	540	5.1	1	30	55 ± 8	1.02 ± 0.1
	130	130	540	4.0	1	31	42 ± 13	1.02 ± 0.1
	135	135	660	2.7 – 4.4	1	32	59 ± 16	1.01 ± 0.1
A-PentOx-A + IND	125	125	720	2.0 – 2.8	0.8	30	49 ± 9	1.19 ± 0.09
+ TEC	130	130	840	2.0 – 2.5	0.6	30	44 ± 12	1.28 ± 0.09
	135	135	960	1.5 – 2.0	0.5	30	46 ± 13	1.28 ± 0.08
A-BuOzi-A	125	125	420	5.1	1	25	48 ± 7	n.a.
+ IND	130	130	480	4.0 – 5.1	1	26	55 ± 9	n.a.
	135	135	540	3.2	1	27	52 ± 9	n.a.

A-BuOzi-A + IND	125	125	600	5.6	1	27	70 ± 10	1.09 ± 0.09
+ TEC	130	130	600	3.6	1	28	97 ± 4	0.97 ± 0.1
	135	135	1080	2.0	0.6	28	89 ± 9	1.12 ± 0.08
A-BuOx-A + IND	125	125	300	5.1	1	25	75 ± 6	n.a.
	130	130	420	4.9	1	26	46 ± 5	n.a.
	135	135	600	3.8	1	27	66 ± 7	1.13 ± 0.07
A-BuOx-A + IND + TEC	125	125	240	6.1	1	28	69 ± 11	
	130	130	420	5.1	1	29	65 ±6	1.28 ± 0.07
	135	135	720	3.0	1	29	64 ± 20	1.25 ± 0.07
A-PentOzi-A + IND	125	125	360	4.8	1	26	79 ±13	n.a.
	130	130	360	4.7 – 5.0	1	26	73 ± 14	n.a.
	135	135	360	4.8	1	27	55 ± 10	n.a.
A-PentOzi-A + IND + TEC	125	125	360	5.4	1	27	71 ± 6	
	130	130	300	5.8	1	28	75 ± 9	1.08 ± 0.10
	135	135	480	4.4	1	29	51 ± 19	1.30 ± 0.05

[a] nozzle temperature; [b] syringe temperature; [c] translation speed; [d] applied voltage; [e] applied pressure; [f] collector temperature; [g] fiber diameter; [h] fiber spacing.

2.10 Dissolution study – sink conditions

Dissolution tests were performed on an in-house built Unites States Pharmacopeia (USP) dissolution apparatus 2 with rotational speed of 50 rpm at 37°C. The dissolution medium was 250 mL phosphate buffered saline (pH = 7.4) (Ph. Eur.) and the printed scaffolds were weighted and added to the pre-heated dissolution medium. At set time points between 0 and 30 min, samples of 1 mL were removed, and the medium was refilled with 1 mL fresh buffer solution (37 °C) every time. The amount of dissolved drug was investigated by UV-Vis spectroscopy at these time points. The data were evaluated using Origin software.

2.11 Melt rheology

Rheological properties of the neat polymers and polymer blends were characterized using a Discovery Hybrid Rheometer HR-2 (TA Instruments, Newcastle, DE, USA) equipped with an Environmental Test Chamber (ETC) and an air chiller system. A plate–plate setup with an upper 25 mm plate was used for the measurements. Flow sweeps of the prepared samples within a shear rate range from 1 to 100 s^{-1} were measured from 180 to 120 °C (for the drug

loaded samples and to 150 °C for the samples without IND) in 5 °C steps. Before every measurement, the samples were equilibrated at the measurement temperature for 10 min. To facilitate comparison of the temperature dependency of different samples, the measured viscosity at a shear rate of 10 s^{-1} was plotted against the temperature. The data were analysed using Origin software.

2.12 Microscopy

The scaffolds were analyzed regarding their fiber spacing and fiber diameter using an Axio Zoom.V16 stereo zoom microscope (Zeiss, Vantaa, Finland) equipped with a Schott VisiLED MC 1100 light (Mainz, Germany). The data acquisition and analysis was conducted using the Zen image processing software version 3.8 (Zeiss, Vantaa, Finland). Fiber diameter was determined on at least 10 fibers and the mean value calculated. To analyze the fiber spacing (if applicable), distances between the stacked fibers in x and y direction was determined in at least 10 pores and mean value was calculated.

3 Results and Discussion

3.1 Polymer synthesis and characterization

In this study, the ABA triblock copolymers pMeOx-*b*-pPentOx-*b*-pMeOx (A-PentOx-A), pMeOx-*b*-pPentOzi-*b*-pMeOx (A-PentOzi-A), pMeOx-*b*-pBuOx-*b*-pMeOx (A-BuOx-A) and pMeOx-*b*-pBuOzi-*b*-pMeOx (A-BuOzi-A) were synthesized via living cationic ring opening polymerization (Figure 1). The synthesis procedure can be found elsewhere[20] and in the Supporting Information (Supporting Information Table S5 – S8, Figure S5 – S8). As the hydrophilic block is the same in all studied polymers, it will be abbreviated with A.

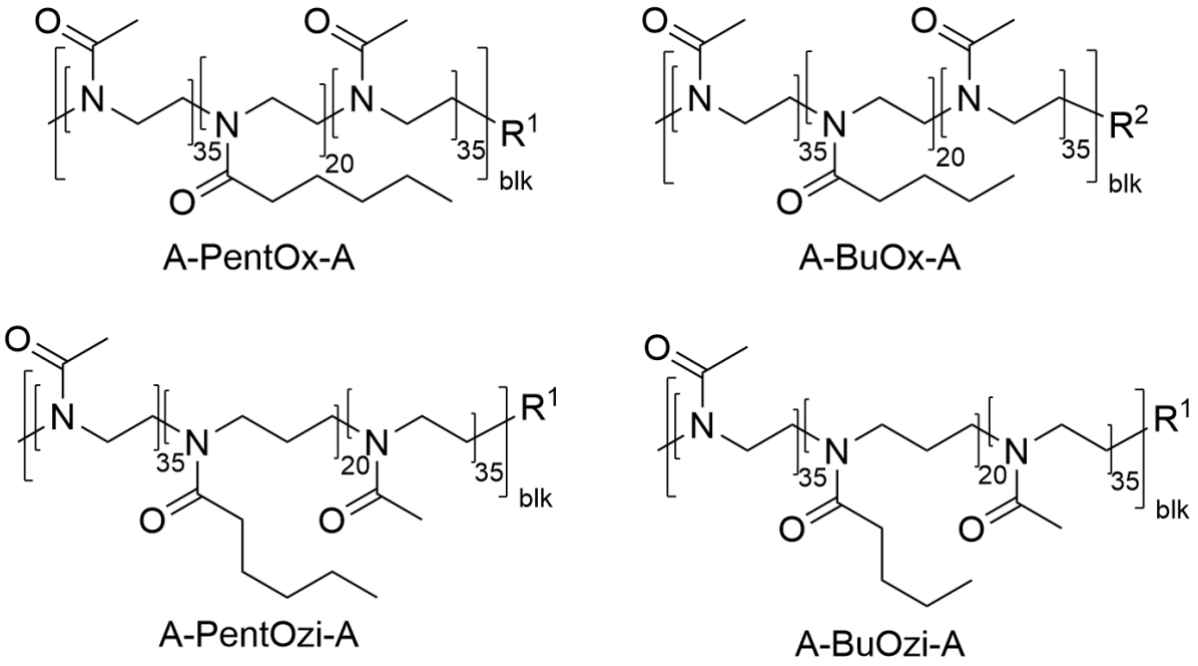

Figure 1. Chemical structures of the polymers A-PentOx-A, A-BuOx-A, A-PentOxi-A and A-BuOzi-A. In the names, A abbreviates the hydrophilic MeOx block, R^1 abbreviates ethyl isonipecotate and R^2 piperidine.

The polymers were characterized by ^{1}H NMR spectroscopy and SEC (Table 4). The molecular weights determined by ^{1}H NMR are in accordance with the theoretical calculated values, whereas the values determined by SEC are overestimated, due to the PMMA calibration used. The low dispersity of the polymers corroborate the rather living character of the polymerization. The only exception shows A-PentOzi-A. The molecular weight determined by ^{1}H NMR is lower than the estimated molecular weight and the SEC elugram shows a bimodal distribution of the polymer and higher dispersity of 1.4, compared to the other polymers. This could result from the modified polymerization procedure used for this reaction, as the polymerization of the hydrophobic PentOzi block did not show any progress in the ^{1}H NMR after 1 week at 120 °C. Increasing the temperature to 150 °C resulted in monomer consumption but apparently led to unwanted side reactions. To the best of our knowledge, the synthesis of ABA triblock

copolymers comprising PentOzi as hydrophobic block was not published before, so no comparison to literature could be done. However, it is known that 2-oxazines suffer from more transfer reactions compared to 2-oxazolines.[49]

Table 4. Overview showing the polymer characteristics of the polymers A-PentOx-A, A-BuOx-A, A-PentOzi-A and A-BuOzi-A, including the theoretical molecular weight ($M_{w,\ theo.}$), the molecular weight determined by ^{1}H NMR spectroscopy ($M_{n,\ NMR}$) and SEC ($M_{n,\ SEC}$) and the dispersity (Đ) of the polymers determined by SEC.

	$M_{w,\ theo.}$ [kg mol^{-1}]	$M_{n,\ NMR}$ [kg mol^{-1}]	$M_{n,SEC}$ [kg mol^{-1}]	Đ
A-PentOx-A	8.9	8.4	13.3	1.2
A-BuOx-A	8.6	8.0	14.7	1.1
A-PentOzi-A	9.2	4.3	10.5	1.4
A-BuOzi-A	9.4	8.1	15.3	1.1

To evaluate the thermal behavior of the polymers and to estimate their printability via MEW, DSC and melt rheology measurements were performed. The A-BuOx-A triblock copolymer showed a single T_g at 61 °C and A-PentOzi-A at 62 °C, whereas the A-BuOzi-A and A-PentOx-A polymers displayed their T_g at 50 °C and 52 °C, respectively (Figure 2A).

The viscosity of the polymers was determined via melt rheology at temperatures between 180 and 150 °C. Flow sweeps were measured with a constant frequency of 10 rad*s^{-1} and increasing shear rate from 1 to 100 s^{-1}. Preliminary experiments ensured that all measurements were done within the linear viscoelastic region (LVE). To better compare the different samples over the whole temperature range, the viscosity value at 10 s^{-1} was plotted against the temperature, as the viscosity value remained constant over the whole shear rate range. This enables a quick comparison of the viscosity at different temperatures and different polymer samples.

As it is to be expected, the polymers showed temperature dependent viscosity (Figure 2B), with decreasing viscosity at increasing temperatures. All measured polymers have a viscosity between 50 and 150 Pa*s in the measured temperature range. Even though the T_g values of A-PentOx-A and A-BuOx-A differ by 9 °C, these two polymers showed a similar viscosity profile. A-BuOzi-A showed the lowest T_g of the studied polymers and the lowest viscosity over the measured temperature range. A different behavior was observed for the measurement of A-PentOzi-A. Here, the viscosity was almost constant over the whole temperature range with only small deviations. This could result from the previously mentioned higher polymer dispersity compared to the other polymers.

In the literature, the viscosity of polymer melts is described to be shear thinning with changes in viscosity over two orders of magnitude within the shear rate range measured here.[50] However, such behavior cannot be observed for the POx/POzi based polymers. On the other hand, the decrease in viscosity with increasing temperature is in line with the results of other polymers studied previously.[51-52]

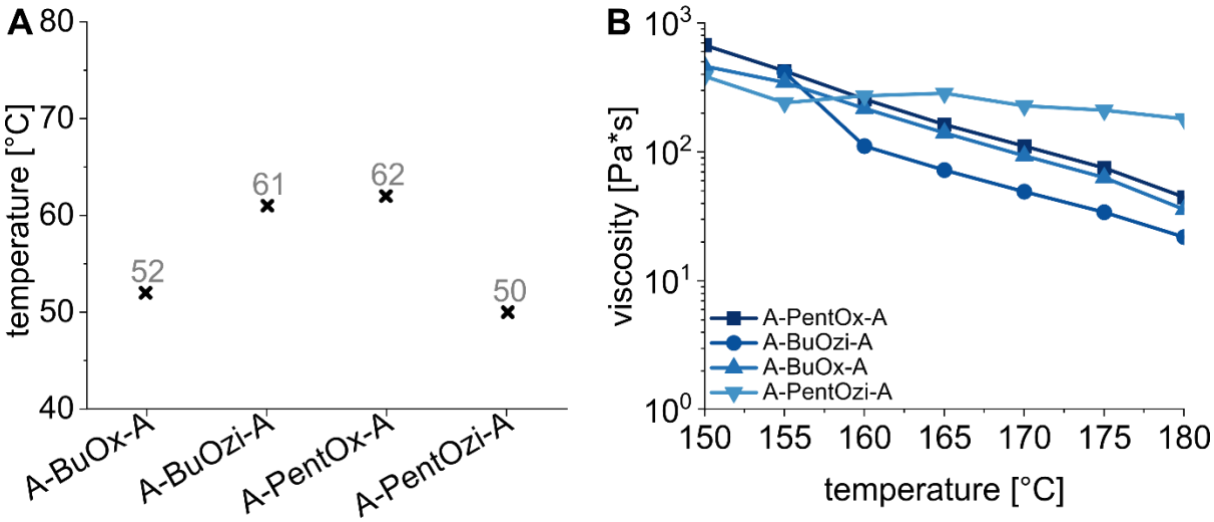

Figure 2. A) Glass transition temperatures and B) melt rheology measurements of the neat polymers A-PentOx-A, A-BuOx-A, A-PentOzi-A and A-BuOzi-A.

Preliminary printing tests via MEW showed, that MEW printing of all four synthesized polymers was not easily achieved. High temperatures (at least 170 °C) were necessary to liquify the polymers sufficiently, similar to our first work on MEW with poly(2-ethyl-2-oxazoline).[53] Additionally, they needed to be kept at such elevated temperature over several hours to successfully remove all air bubbles within the polymer melt. Heating the polymer over long time resulted in discoloration and therefore probably partial degradation of the polymers, despite working under N_2 atmosphere. Therefore, it was decided to investigate the influence of different plasticizers on the thermal and viscoelastic properties of the polymers and investigate the influence of the plasticizers on the printability of the polymers. In the following, citrate-based, acetyl-based and glycol-based plasticizers are investigated and their influence on the polymer's thermal properties and viscosity is discussed. To the best of our knowledge, the effect of plasticizers on poly(2-oxazoline)s and poly(2-oxazine)s in general and ABA triblock copolymer in particular has not been studied to date.

3.2 Characterization and printability assessment of ABA triblock copolymers with plasticizer

To analyze the influence of plasticizers on the polymer viscosity, first, samples comprising the polymer A-PentOx-A and 5 wt% plasticizer were prepared, and flow sweeps at different temperatures were measured (Figure 3A). Depending on the influence of the plasticizers on the viscosity and printability on A-PentOx-A, the selection of plasticizers was reconsidered and reduced.

The addition of citric acid to A-PentOx-A resulted in an increase in viscosity compared to the neat polymer. This could be explained by the formation of H-bridges between the plasticizer's acid groups and the polymers amide groups. Through the presence of three acid groups per citric acid molecule, physical crosslinking between polymer and plasticizer could occur, leading to an increase in the viscosity values. While this suggested interaction between A-PentOx-A and citric acid was not further investigated, a decrease in viscosity was observed when triacetin, ethylene glycol or triethyl citrate were added. Due to the chemical structure of the polymers and the plasticizers, no stronger interactions between polymer and plasticizer, such as H-bonding, can be expected.

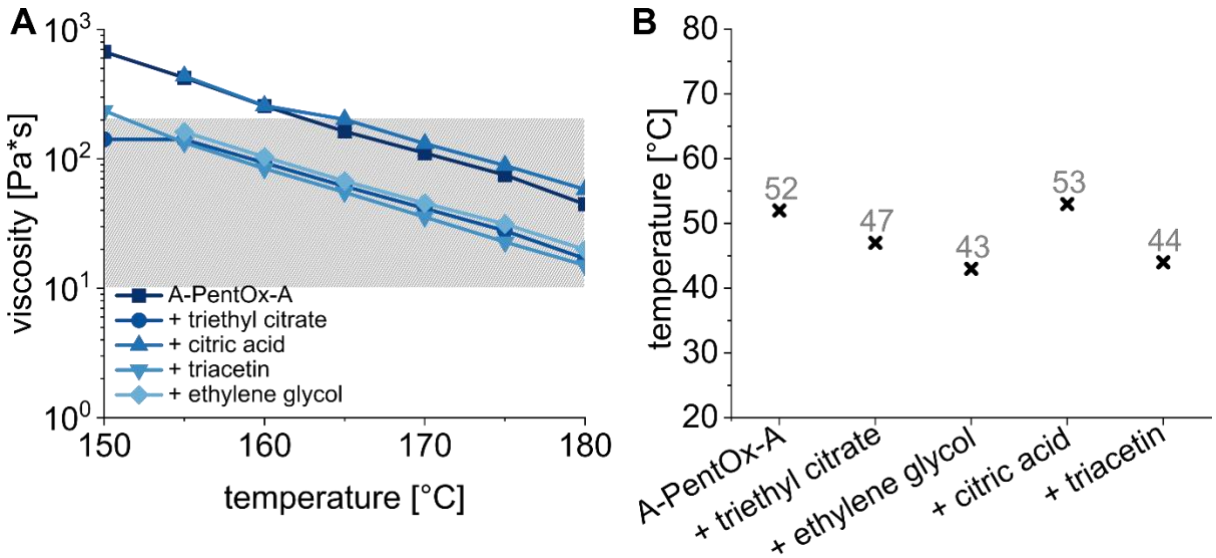

Figure 3. A) Melt rheology measurements of A-PentOx-A and the polymer mixed with different plasticizers in the temperature range from 150 to 180 °C and B) glass transition temperatures of these blends. The grey background in A shows the area, wherein the samples are estimated to be printable via MEW; the area was chosen based on previous printing tests and should only be considered as a guide for the eye for the reader.

A dependency of plasticizer on the polymer properties was also observed in the T_g of the polymer-plasticizer blends (Figure 3B). The addition of triethyl citrate, triacetin and ethylene glycol resulted in a decrease of the T_g from 52 °C to 47 – 42 °C, respectively, whereas the addition of citric acid increased the T_g slightly to 53 °C.

Based on the viscosity and T_g measurements, addition of triethyl citrate, triacetin and ethylene glycol clearly plasticize the polymer blends compared to the neat samples. The observed effect is often explained by free volume theory, which states, that plasticizers, usually small molecules with low T_g values themselves, act by penetrating between and thus, separating the polymer chains, reducing the intermolecular forces between the polymer chains.[54] This leads to an increase in free volume, a decrease in T_g and an increase in mobility of polymer segments.[37]

To test the printability of the polymer plasticizer blends, scaffolds with 1.5 mm spacing and 10 layers in each direction (0° and 90° fiber orientation) were fabricated via MEW. When comparing the printability of A-PentOx-A-plasticizer blends, it was observed that the addition of citric acid did not result in a printable polymer blend, independent of the fabrication temperature used. Therefore, this plasticizer was excluded from further studies. The samples containing triethyl citrate, triacetine and ethylene glycol were processed from 155 °C to 165 °C (Figure 4). Below 155 °C, neither of the samples showed good adhesion on the print bed and the fibers were not adhering to each other. Increasing the temperature to 155 °C resulted in good fiber stacking for the sample containing triethyl citrate, whereas the triacetin and ethylene glycol containing polymer samples showed poor fiber attachment in the first layers, leading to overall poor fiber stacking even in the higher layers. Increasing the temperature to 160 °C resolved the issue of poor fiber attachment in the ethylene glycol containing sample. Interestingly, a further increase of temperature to 165 °C did not result in fiber production of the triacetin containing samples. It was observed that keeping the polymer plasticizer mixture at elevated temperature over several hours resulted in phase separation between polymer and plasticizer (not observed during rheological studies). Due to the phase separation of triacetin and polymer and the overall better printability of triethyl citrate and ethylene glycol, triacetin was not investigated further. For the samples containing ethylene glycol or triethyl citrate, a further increase in temperature was possible, but this increases the potential for polymer degradation. Apart from lowering the print temperature, triethyl citrate apparently supports the stacking of the fibers while printing. Consequently, melt rheology and printability tests for A-BuOx-A, A-BuOzi-A and A-PentOzi-A were conducted with triethyl citrate and ethylene glycol as additives.

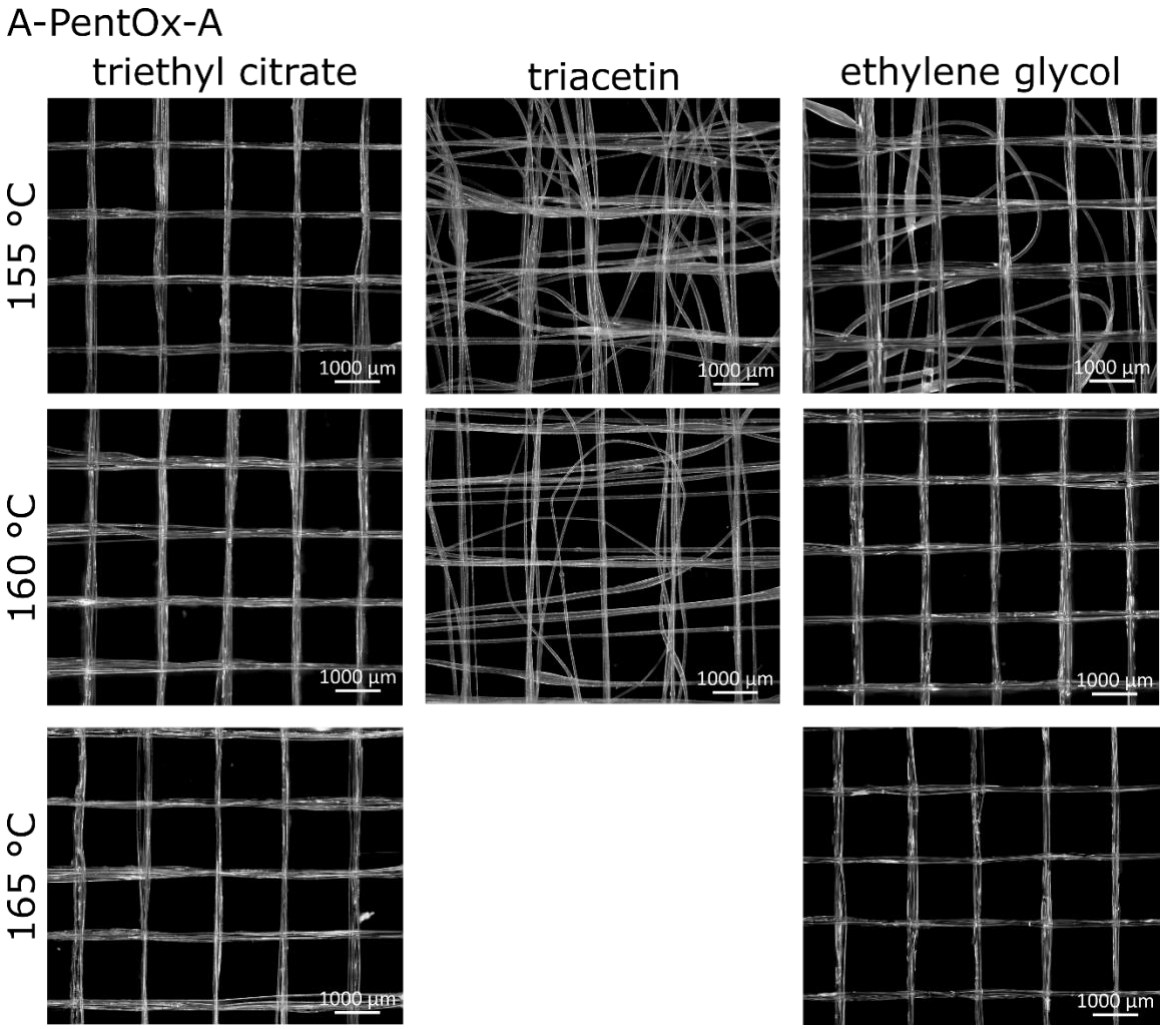

Figure 4. Microscopy pictures of scaffolds printed via MEW (10 layers, 1.5 mm fiber spacing) with polymer and plasticizer blends containing A-PentOx-A and triethyl citrate, triacetin and ethylene glycol, respectively. Below 155 °C no adhesion of the fibers to the collector plate was observed. In the sample containing triacetin phase separation between the polymer and plasticizer did not result in printable samples at 165 °C.

The samples containing A-BuOx-A and A-BuOzi-A and A-PentOzi-A with triethyl citrate or ethylene glycol as plasticizers showed a similar trend in the melt rheology measurements as observed for A-PentOx-A (Figure 5A - C). The polymer viscosity was decreasing with the addition of the plasticizer. However, for all three polymers, a more pronounced difference between triethyl citrate and ethylene glycol was observed, compared to the A-PentOx-A sample. For A-PentOzi-A and A-BuOzi-A, triethyl citrate resulted in a lower viscosity compared to ethylene glycol. However, A-BuOx-A showed the inverse trend, here the addition of ethylene glycol resulted a comparably lower viscosity.

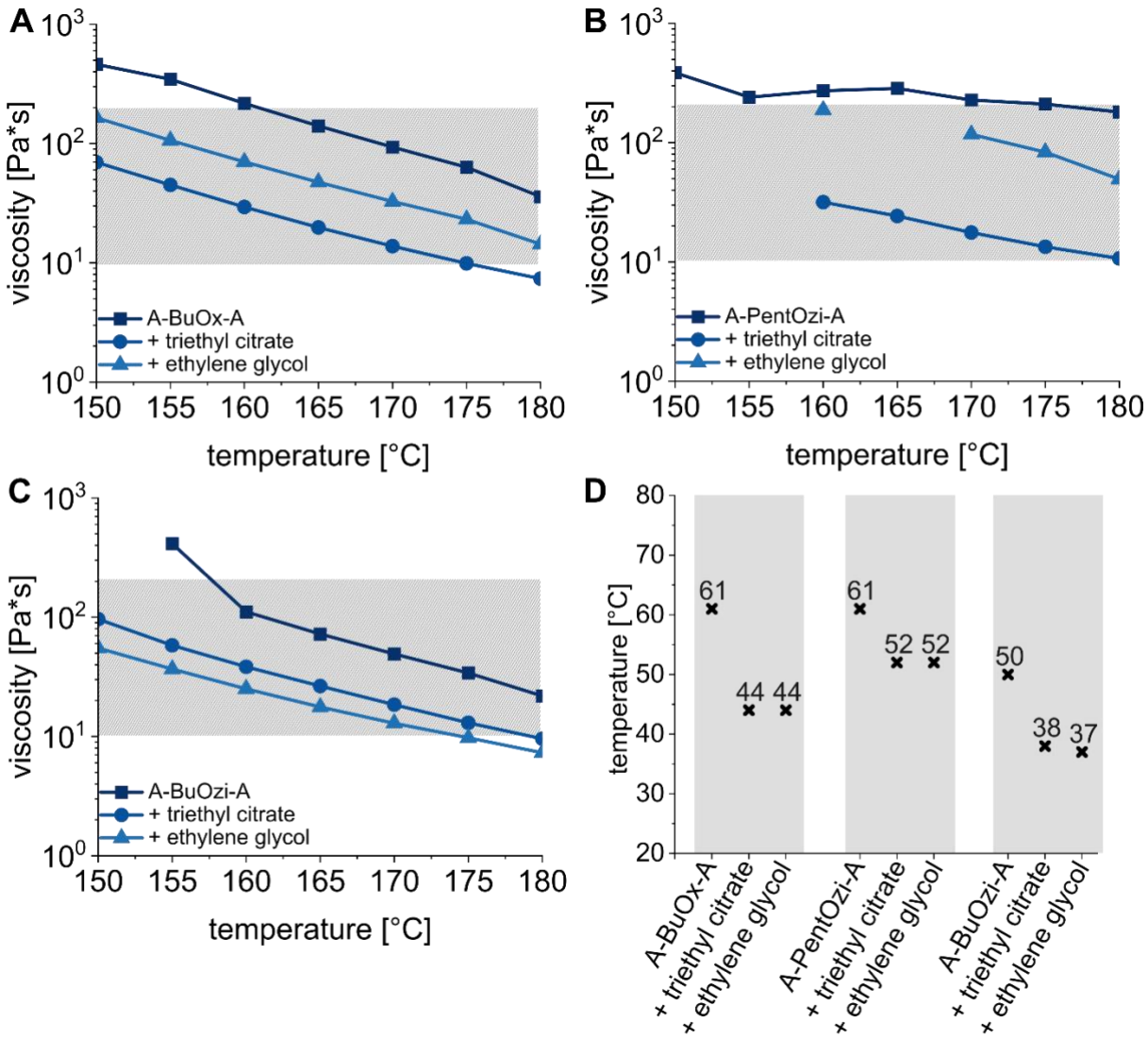

Figure 5. A-C) Melt rheology measurements in the temperature range from 150 to 180 °C for neat polymers and the polymer-plasticizers blends for A-BuOx-A (A), A-PentOzi-A (B) and A-BuOzi-A (C). The grey background shows the area, wherein the samples should be printable via MEW; the area was chosen based on previous printing tests and should only be considered as a guide for the eye for the reader. D) Glass transition temperatures of these blends.

Smaller differences compared to A-PentOx-A were observed in the T_g values of the neat polymers and the polymer-plasticizer blends (Figure 5D). For the samples comprising A-PentOx-A a deviation of the T_g values of 4 °C was observed, depending on whether either triethyl citrate or ethylene glycol was used, whereas for A-BuOx-A, A-PentOzi-A and A-BuOzi-A, the same or essentially same T_g of 44 °C, 52 °C and 38/37 °C, respectively, was observed.

Despite the minimal differences in T_g, processability was affected rather markedly. The printability of A-BuOzi-A showed a similar result to A-PentOx-A (Supporting Information Figure S10). Starting from 155 °C, fiber extrusion was achieved, however, for both plasticizers poor fiber attachment to the collector plate was observed, resulting in overall bad print quality. By

increasing the temperature to 160 °C, the fibers stuck on the collector plate and box-like structures with reasonably good fiber stacking can be observed, with improved fiber stacking for the samples containing ethylene glycol. Further increasing the temperature to 165 °C resulted in better fiber stacking for triethyl citrate. A different behavior was observed for A-BuOx-A and the plasticizers (Supporting Information Figure S11). Here, phase separation between the polymer and triethyl citrate was observed, preventing fiber extrusion during the print process (Supporting Information Figure S12). In contrast, the addition of ethylene glycol led to a printable blend from 160 °C and a further temperature increase to 165 and 170 °C resulted in improved fiber stacking. Even though the viscosity of A-BuOx-A was found comparable to A-PentOx-A, clear differences in printability were observed. Testing the printability of A-PentOzi-A with the plasticizers, resulted in polymer extrusion from 160 °C, but poor fiber attachment to the collector plate (Supporting Information Figure S13). Increasing the print temperature to 170 °C resolved the problem.

The printing parameters, such as applied collector speed and applied voltage, had to be adjusted for every polymer-plasticizer blend separately, which makes it difficult to observe clear trends depending on the plasticizer and polymer used (Table 2). However, for all polymer-plasticizer blends it was observed, that increasing the temperature led to an increase in applied collector speed due to the decreasing viscosity of the blends. For instance, for A-PentOx-A with triethyl citrate, the maximal collector speed increased from 540 mm*min^{-1} to 780 mm*min^{-1} with the temperature increasing from 155 °C to 165 °C. For A-BuOzi-A and triethyl citrate a maximal collector speed of 420 mm*min^{-1} was used, and for A-PentOzi-A and triethyl citrate it was only 180 mm*min^{-1}, due to the fast solidification of the produced fiber.

Considering all the results obtained for the four polymers with triethyl citrate and ethylene glycol as plasticizers, minor differences between the plasticizers were observed in the temperature dependent viscosity and T_g values, but the overall printability of the samples containing triethyl citrate was better, due to improved fiber stacking. The exception was A-BuOx-A, for which phase separation between triethyl citrate and the polymer was observed during the printing process. However, preliminary printing tests for the ternary blend of A-BuOx-A, triethyl citrate and the model drug IND did not show phase. Therefore, it was decided to continue the study with triethyl citrate.

3.3 Characterization and printability assessment of ABA triblock copolymers with triethyl citrate and IND

As not only the addition of a plasticizer, but also the addition of a small molecule drug can influence the viscosity of a polymer melt (as they might act as plasticizers themselves), flow

sweeps of the polymer-drug blends were measured, and the printability was tested. Interestingly, by the addition of 50 wt% IND to the A-PentOx-A sample, the viscosity dropped by two orders of magnitude (Figure 6A). Additionally, the viscosity of the sample could now be monitored down to a temperature of 120 °C. By the addition of triethyl citrate (5 wt%) to the polymer-drug blends, an additional, but minor decrease in viscosity was observed. A similar trend was observed for the sample containing A-PentOzi-A as polymer excipient (Figure 6C). The viscosity was highly influenced by the addition of either the plasticizer or the drug, the combination of both resulted just in a minor drop compared to the IND containing sample. In these samples IND has a bigger influence on the melt viscosity than the additionally used plasticizer. However, the added plasticizer influences the printability of the polymer-drug blends, which will be discussed below. In particular, it needs to be considered, that the amount of triethyl citrate added to the blend was only 5 wt%, whereas 50 wt% of the drug was added. As the small molecule drug is acting as a plasticizer as well, the greater influence on the polymer resulting from the larger amount added to the blend can be expected. Further increasing the drug content of the blend would lead to lower viscosity at elevated temperatures, but probably also to supersaturated ASDs with the risk of the drug not fully dissolving in the polymer matrix leading to residual drug crystallites in the ASD or accelerated drug crystallization from the oversaturated blends.

Interestingly, for the blends comprising A-BuOx-A and A-BuOzi-A (Figure 6B, D), the addition of the drug resulted in a decrease of the viscosity of approximately one order of magnitude, while the addition of drug and plasticizer resulted in a further decrease, larger than observed for A-PentOx-A and A-PentOzi-A.

Even though there were small differences in the viscosity measurements, all polymers showed a viscosity below 110 Pa*s at 125 °C for the samples containing drug and plasticizer and 130 °C for the samples containing only the drug.

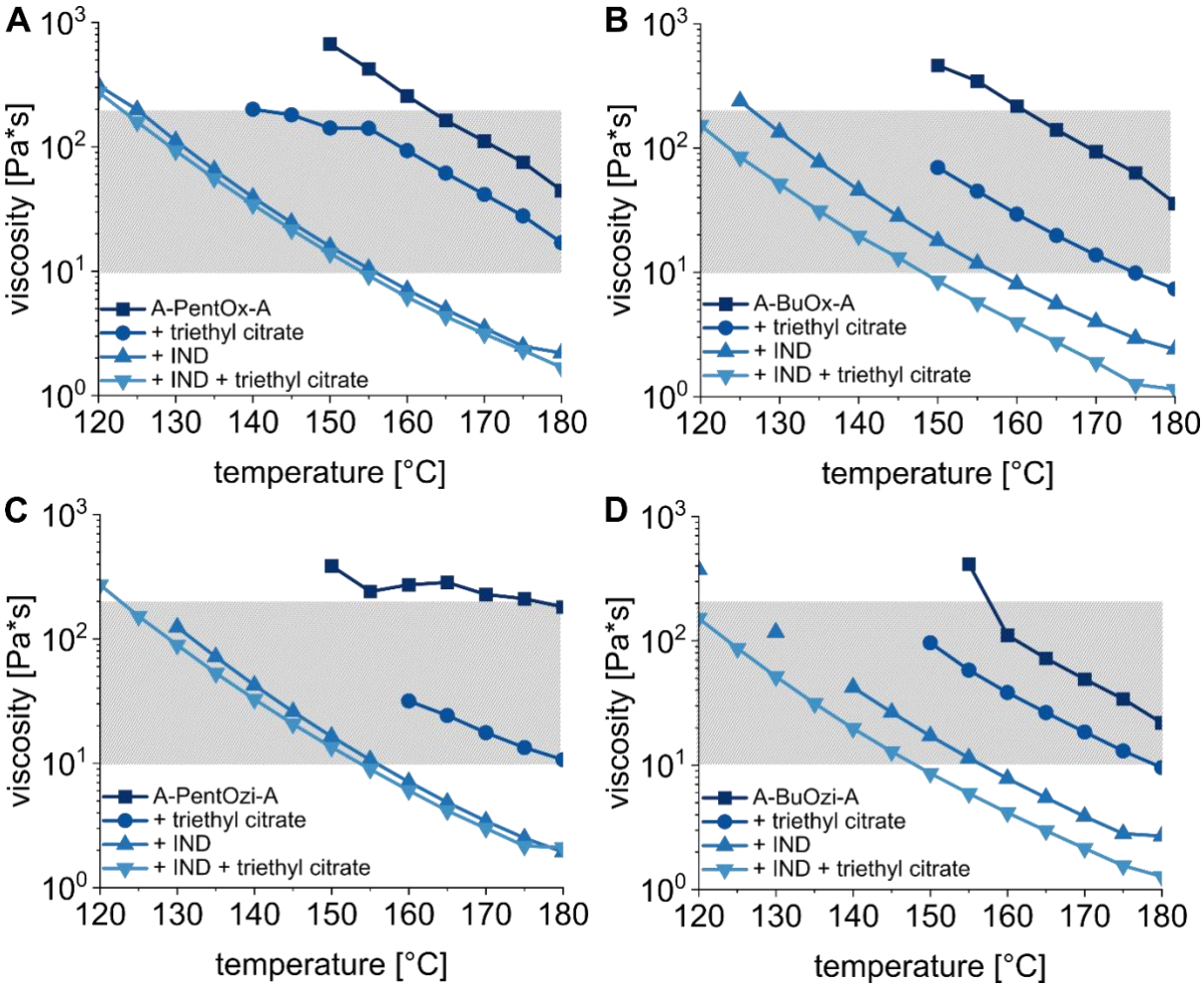

Figure 6. Melt rheology measurements of the neat polymers, the polymers-drug or plasticizer blends and the polymers-drug-plasticizer blends in the temperature range from 120 to 180 °C for A-PentOx-A (A), A-BuOx-A (B), A-PentOzi-A (C) and A-BuOzi-A (D). The grey background shows the area, wherein the samples should be printable via MEW, but should only be considered a rough guide for the eye.

In addition to the melt viscosity, the T_g of the above-mentioned samples was studied (Figure 7). As already mentioned above, the T_g of the neat polymers ranged between 50 and 61 °C and the addition of triethyl citrate as plasticizer reduced the T_g by 5 to 17 °C, depending on the polymer used. By addition of IND to the polymer, a less pronounced decrease of 2 - 8 °C in the T_g values was observed, which resulted in T_g values of the polymer-drug blends between the T_g of the neat polymers and IND (T_g = 43 °C).

Our results indicate that the plasticizer had a bigger influence on the T_g of the sample, whereas the drug had a bigger influence on the polymer viscosity. If now both, the drug and plasticizer were present in the sample, a remarkable decrease in the T_g values was observed for all polymers. Here, the T_g was decreased by 13 – 34 °C compared to the neat polymer. For the sample containing A-PentOzi-A, IND and the plasticizer, the drop in T_g should be considered especially critical, as the resulting T_g was with 27 °C just slightly above room temperature.

This can result in problems in sample preparation, as reported previously due to the viscous and sticky nature of the blend.[15] In general, all printed drug-loaded scaffolds showed hygroscopic character and had to be stored at low humidity to prevent water absorption and the samples getting sticky, which made handling challenging. On the other side, for using them as sublingual drug delivery vehicle, the hygroscopic character is beneficial, as it would allow the scaffold to stick in the mouth floor or the cheek while dissolving and releasing the drug.

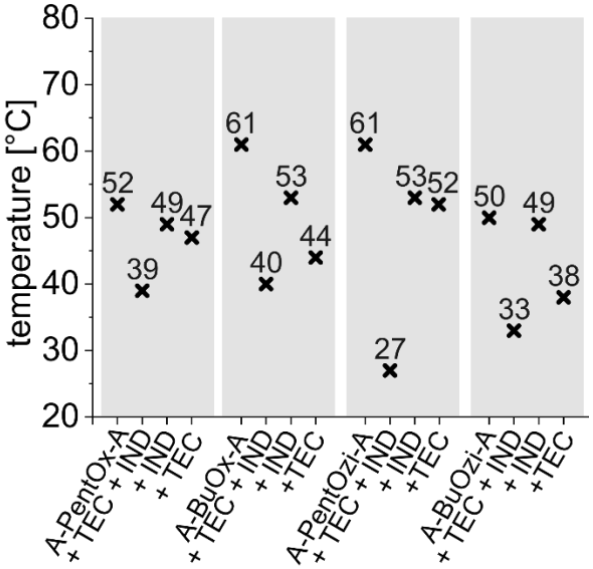

Figure 7. Glass transition temperatures of the neat polymers, the polymers mixed with drug or plasticizer and the polymers mixed with drug and plasticizer for A-PentOx-A, A-BuOx-A, A-PentOzi-A and A-BuOzi-A. The used drug is indomethacin (IND), and the plasticizer is triethyl citrate (TEC).

Comparable to the fiber meshes printed with the polymer-plasticizer blends, drug loaded samples were fabricated into scaffolds with 10 layers in each direction (0° and 90° fiber orientation) and 1.5 mm fiber spacing. MEW printing was tested by increasing the temperature in 5 °C steps until fiber extrusion was observed. When testing the printability of the samples containing polymer and IND with and without plasticizer, it was observed that all samples, except A-PentOzi-A, were printable from 125 °C onwards (Figure 8, Supporting Information Figure S14 – S16). The best stacking was achieved at either 130 °C or 135 °C, depending on the polymer. Additionally, the fiber stacking of the samples containing triethyl citrate was overall better than for the samples without the plasticizer.

In the samples without the plasticizer, the fiber attachment to the collector plate in the first layers was poor, resulting in an overall reduced print quality. At 125 °C the solidification of the polymer melt was too fast to get a proper attachment of the first drop of polymer melt on the collector plate from where the continuous fiber can be formed. Additionally, it was observed, that printing at 120 °C and 125 °C resulted in scaffolds with poor interlayer adhesion,

presumably due to the rapid melt solidification. To overcome this issue, printing tests for the samples without added plasticizer were performed at 130 °C and 135 °C, resulting in better attachment of the first layer on the collector plate. However, the overall fiber stacking remained poor, potentially caused by electrostatic repulsion of the fibers due to ionizable IND.

For the samples containing additional plasticizer, scaffolds still showed poor print quality due to poor fiber stacking at a print temperature of 125 °C, but increasing the temperature to 130 °C or 135 °C improved the fiber stacking. For all the tested samples, it appeared, that a melt viscosity of approximately 100 Pa*s resulted in the best printing quality in terms of fiber stacking. Importantly, the addition of the plasticizer did not markedly reduced the print temperature, but ensured a better stacking of the deposited microfibers.

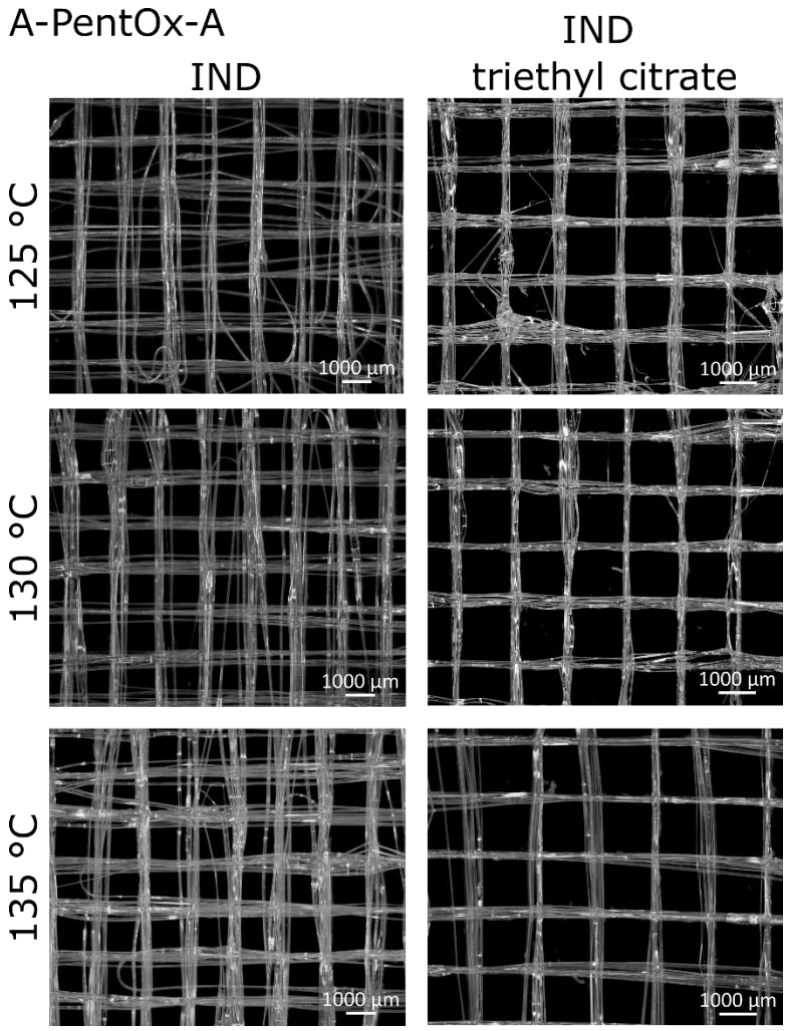

Figure 8. Microscopy images of the printability tests via MEW (10 layers, 1.5 mm fiber spacing) of A-PentOx-A - IND blends with and without the plasticizer triethyl citrate at 125, 130 and 135 °C.

Apart from fiber stacking, the applicable collector speed depended on whether the plasticizer was added or not. However, as discussed before, the print parameters had to be adjusted for

each sample separately. In general, adding triethyl citrate and increasing the print temperature allowed for an increased translation speed for all drug loaded samples (Table 3). The only exception was A-PentOzi-A, for which the applied translation speed was constant at 360 mm*min^{-1} for all tested temperatures without plasticizer. By adding the plasticizer, the speed could be increased to 480 mm*min^{-1} at 135 °C.

To confirm the fully amorphous nature of the printed samples even at 125 °C print temperature, which is well below the melt temperature of IND (160 °C), thermograms of the IND loaded scaffolds with and without plasticizer were recorded (Supporting Information Figure S18). The clear absence of an IND melting peak suggests a fully amorphous character of the scaffolds.

Compared to the previously published study on the fabrication of IND loaded microfibers fabricated via MEW with a POx/POzi based polymer system, we were not able to lower the fabrication temperature significantly (135 °C in the previous study for 50 wt% IND loading).[15] However, we were able to prepare a polymer-drug-plasticizer system, which does not require additional hot melt extrusion to obtain sufficient mixing of the components and even after several hours at the printing temperature, no indicators of drug degradation, either visibly (indicated by discoloration) or by ^{1}H NMR spectra of the printed scaffolds were observed (Supporting Information Figure S17).

3.4 Dissolution testing of the drug loaded microfiber scaffolds

Not only the amount of added drug can alter the dissolution profile of the scaffolds, but also the added plasticizer.[38, 55-56] To determine the influence of the plasticizer on the dissolution profile, scaffolds with and without added triethyl citrate were printed and their dissolution profile under sink conditions monitored (Figure 9). For the sample containing A-BuOzi-A, no plasticizer influence was observed, as the samples with and without triethyl citrate dissolved fully within the first 3 min of the experiment and reached a plateau at 100% drug release shortly after. On the contrary, for the A-BuOx-A and A-PentOzi-A based scaffolds, the addition of the plasticizer resulted in a slower dissolution compared to the scaffolds without. Without the plasticizer, the scaffolds were dissolved within approximately 2.5 min, whereas the addition of plasticizer extended the dissolution time to 30 min. For the samples containing A-PentOx-A, identical behavior between the samples was observed in the first 5 min of the experiment independent on the addition of plasticizer, but after 6 min a drop to 60% drug concentration was determined for the sample with plasticizer, whereas the samples without plasticizer showed a drop to 80% drug concentration. This was probably caused by partial precipitation of the drug or coacervation of the drug with the polymer. However, this could not be visually confirmed.

In the literature, different dissolution behaviors were described when adding a plasticizer to a polymer-drug blend. For some polymer-drug-plasticizer blends, the addition of the plasticizer resulted in faster drug release, probably due to weakening of the polymer-polymer interaction.[38] For other systems, no influence was observed,[55] or even the inverse behavior, where the addition of a plasticizer resulted in longer dissolution time.[56] This makes it difficult to predict the influence of the plasticizer on the polymer blend and its dissolution. Here, polymers of the same polymer class but with different hydrophobicity of the polymer middle block were used, revealing different influence of the plasticizer on the printed scaffolds in the dissolution tests, which makes it necessary to investigate the influence of the plasticizer for every blend separately.

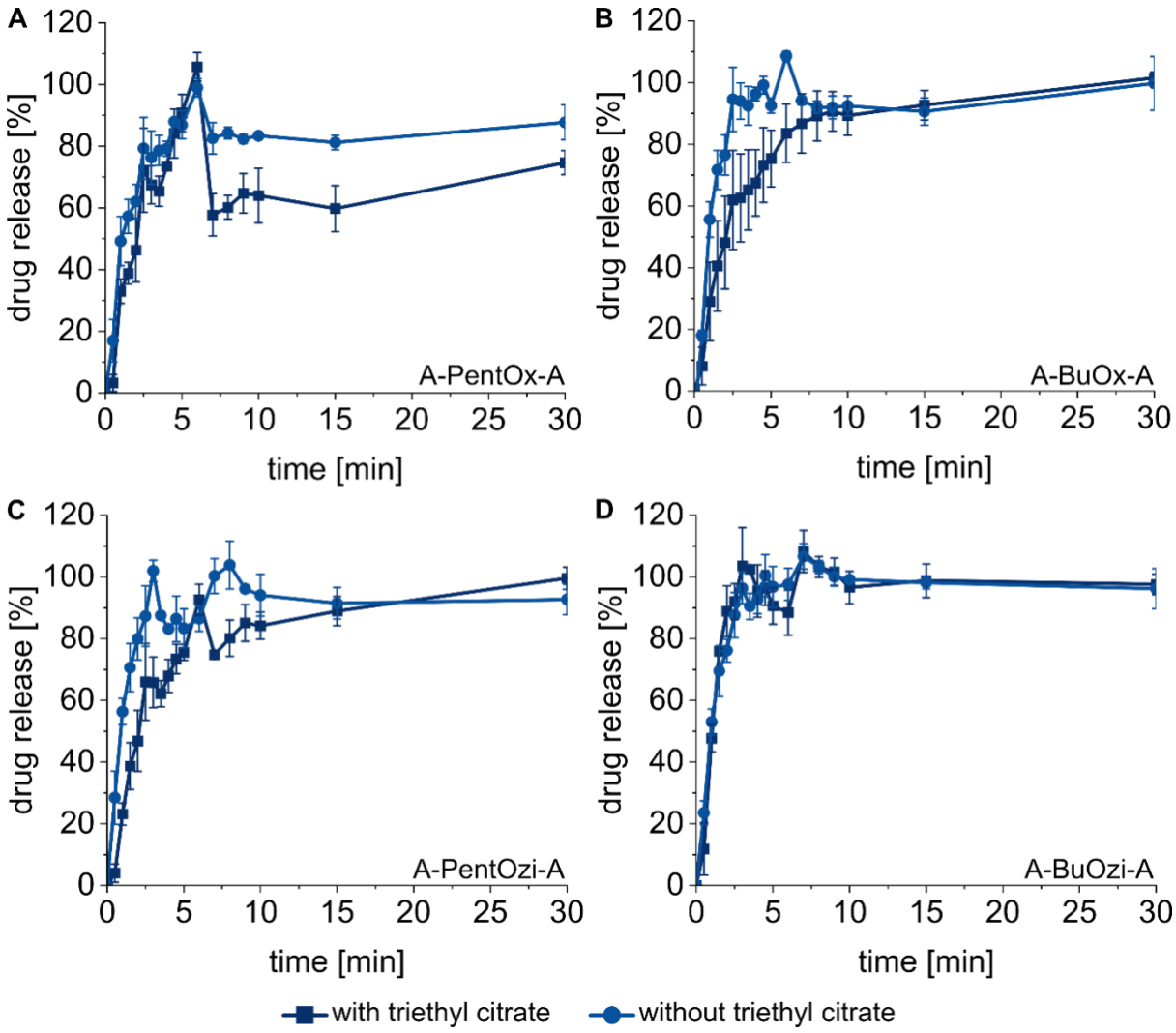

Figure 9. Dissolution profiles (sink conditions, PBS, pH = 6.8) of the IND loaded microfiber scaffolds with and without the added plasticizer triethyl citrate. The polymers used are A-PentOx-A (A), A-BuOx-A (B), A-PentOzi-A (C) and A-BuOzi-A (D).

4 Conclusion

In this study, the influence of plasticizers on four poly(2-oxazoline) and poly(2-oxazine) based ABA triblock copolymers to decrease the fabrication temperature via MEW was studied. The addition of triethyl citrate and ethylene glycol resulted in printable polymer blends with improved fiber stacking for the blends comprising triethyl citrate. Through the addition of the model drug IND, the fabrication temperature could be decreased to 130 °C, reducing the risk of degradation of both, drug and polymer. The addition of triethyl citrate did support the fiber stacking of the drug loaded microfibers. Interestingly, the addition of the plasticizer influenced the dissolution profile of the scaffolds differently depending on the polymer used, despite the very similar chemical structure of different polymers. Our results provide a starting point to better understand and optimize drug loaded and rapidly dissolving microfiber scaffolds.

In the present study, the polymer-drug blends were printable without the added plasticizer, as IND itself acted as plasticizer in the mixture. Therefore, the improved fiber stacking is the primary benefit of adding triethyl citrate. For IND as a model drug, the addition of the plasticizer is optional, whereas preliminary tests with other drugs indicate that the use of a plasticizer to decrease the viscosity of the polymer-drug blends is important to obtain blends that can be fabricated via MEW. This is currently explored in more detail and will be reported in due time.

Acknowledgement

Th authors acknowledge financial support by the Academy of Finland (Grant no. 337660 and Grant no. 342983). The authors thank Sami-Pekka Hirvonen for SEC measurements, Mengshi Yang and Christian May for providing A-BuOx-A. The authors thank Prof. Dietmar Hutmacher and Peter Bate for their support in providing the custom-build MEW.

Conflict of Interest

R. L. is listed as inventor on patents and patent applications pertinent to some materials discussed in this contribution and is co-founder of DelAQUA Pharmaceuticals, intending to commercialize poly(2-oxazoline) based drug formulations.

CRediT authorship contribution statement

L. Keßler: Conceptualization, Investigation, Visualization, Data curation, Writing – original draft; R. Luxenhofer: Conceptualization, Funding acquisition, Writing – review & editing, Supervision. All authors have read and agreed to the published version of the manuscript.

References

[1] U. E. Illangakoon, H. Gill, G. C. Shearman, M. Parhizkar, S. Mahalingam, N. P. Chatterton, G. R. Williams Fast dissolving paracetamol/caffeine nanofibers prepared by electrospinning *Int J Pharm* **2014**, *477*, 369-379.

[2] D. Harris, J. R. Robinson Drug delivery via the mucous membranes of the oral cavity *J Pharm Sci* **1992**, *81*, 1-10.

[3] V. Hearnden, V. Sankar, K. Hull, D. V. Juras, M. Greenberg, A. R. Kerr, P. B. Lockhart, L. L. Patton, S. Porter, M. H. Thornhill New developments and opportunities in oral mucosal drug delivery for local and systemic disease *Adv Drug Deliv Rev* **2012**, *64*, 16-28.

[4] M. T. Sheu, C. M. Hsieh, R. N. Chen, P. Y. Chou, H. O. Ho Rapid-Onset Sildenafil Sublingual Drug Delivery Systems: In Vitro Evaluation and In Vivo Pharmacokinetic Studies in Rabbits *J Pharm Sci* **2016**, *105*, 2774-2781.

[5] S. Baghel, H. Cathcart, N. J. O'Reilly Polymeric Amorphous Solid Dispersions: A Review of Amorphization, Crystallization, Stabilization, Solid-State Characterization, and Aqueous Solubilization of Biopharmaceutical Classification System Class II Drugs *J Pharm Sci* **2016**, *105*, 2527-2544.

[6] A. B. Anane-Adjei, E. Jacobs, S. C. Nash, S. Askin, R. Soundararajan, M. Kyobula, J. Booth, A. Campbell Amorphous solid dispersions: Utilization and challenges in preclinical drug development within AstraZeneca *Int J Pharm* **2022**, *614*, 121387-121402.

[7] A. Singh, Z. A. Worku, G. Van den Mooter Oral formulation strategies to improve solubility of poorly water-soluble drugs *Expert Opin Drug Deliv* **2011**, *8*, 1361-1378.

[8] G. Van den Mooter, M. Wuyts, N. Blaton, R. Busson, P. Grobet, P. Augustijns, R. Kinget Physical stabilisation of amorphous ketoconazole in solid dispersions with polyvinylpyrrolidone K25 *Eur J Pharm Sci* **2001**, *12*, 261-269.

[9] U. S. Kestur, L. S. Taylor Role of polymer chemistry in influencing crystal growth rates from amorphous felodipine *CrystEngComm* **2010**, *12*, 2390-2397.

[10] T. Xie, L. S. Taylor Dissolution Performance of High Drug Loading Celecoxib Amorphous Solid Dispersions Formulated with Polymer Combinations *Pharm Res* **2016**, *33*, 739-750.

[11] J. T. Morott, M. Pimparade, J. B. Park, C. P. Worley, S. Majumdar, Z. Lian, E. Pinto, Y. Bi, T. Durig, M. A. Repka The effects of screw configuration and polymeric carriers on hot-melt extruded taste-masked formulations incorporated into orally disintegrating tablets *J Pharm Sci* **2015**, *104*, 124-134.

[12] A. Agrawal, M. Dudhedia, W. Deng, K. Shepard, L. Zhong, E. Povilaitis, E. Zimny Development of Tablet Formulation of Amorphous Solid Dispersions Prepared by Hot Melt Extrusion Using Quality by Design Approach *AAPS PharmSciTech* **2016**, *17*, 214-232.

[13] H. Wu, Y. Liu, T. Ci, X. Ke Application of HPMC HME polymer as hot melt extrusion carrier in carbamazepine solid dispersion *Drug Dev Ind Pharm* **2020**, *46*, 1911-1918.

[14] R. Svoboda, M. Nevyhostena, J. Machackova, J. Vaculik, K. Knotkova, M. Chromcikova, A. Komersova Thermal degradation of Affinisol HPMC: Optimum Processing Temperatures for Hot Melt Extrusion and 3D Printing *Pharm Res* **2023**, *40*, 2253-2268.

[15] L. Keßler, Z. Mirzaei, J. C. Kade, R. Luxenhofer Highly Porous and Drug-Loaded Amorphous Solid Dispersion Microfiber Scaffolds of Indomethacin Prepared by Melt Electrowriting *ACS Appl Polym Mater* **2023**, *5*, 913-922.

[16] S. Feng, S. Bandari, M. A. Repka Investigation of poly(2-ethyl-2-oxazoline) as a novel extended release polymer for hot-melt extrusion paired with fused deposition modeling 3D printing *J Drug Deliv Sci Technol* **2022**, *74*, 103558-103567.

[17] L. Keßler, R. Mishra, S. Hietala, M. Lammens, T. Rades, B. van Veen, A. Juppo, T. Laaksonen, C. Strachan, R. Luxenhofer Amorphous solid dispersions of amphiphilic polymer excipients and indomethacin prepared by hot melt extrusion *ChemRxiv* **2024**. DOI: 10.26434/chemrxiv-2024-45fhm

[18] M. S. Haider, R. Luxenhofer Development of Poly (2-oxazoline) s and poly (2-oxazine) s based formulation library and estimation of polymer/drug compatibility *ChemRxiv* **2022**. DOI: 10.26434/chemrxiv-2022-s8xc3
[19] M. S. Haider, M. M. Lübtow, S. Endres, S. Forster, V. J. Flegler, B. Bottcher, V. Aseyev, A. C. Poppler, R. Luxenhofer Think Beyond the Core: Impact of the Hydrophilic Corona on Drug Solubilization Using Polymer Micelles *ACS Appl Mater Interfaces* **2020**, *12*, 24531-24543.
[20] M. M. Lübtow, M. S. Haider, M. Kirsch, S. Klisch, R. Luxenhofer Like Dissolves Like? A Comprehensive Evaluation of Partial Solubility Parameters to Predict Polymer-Drug Compatibility in Ultrahigh Drug-Loaded Polymer Micelles *Biomacromolecules* **2019**, *20*, 3041-3056.
[21] M. M. Lübtow, L. Kessler, A. Appelt-Menzel, T. Lorson, N. Gangloff, M. Kirsch, S. Dahms, R. Luxenhofer More Is Sometimes Less: Curcumin and Paclitaxel Formulations Using Poly(2-oxazoline) and Poly(2-oxazine)-Based Amphiphiles Bearing Linear and Branched C9 Side Chains *Macromol Biosci* **2018**, *18*, 1800155-1800171.
[22] D. Hwang, N. Vinod, S. L. Skoczen, J. D. Ramsey, K. S. Snapp, S. A. Montgomery, M. Wang, C. Lim, J. E. Frank, M. Sokolsky-Papkov, Z. Li, H. Yuan, S. T. Stern, A. V. Kabanov Bioequivalence assessment of high-capacity polymeric micelle nanoformulation of paclitaxel and Abraxane(R) in rodent and non-human primate models using a stable isotope tracer assay *Biomater* **2021**, *278*, 121140-121150.
[23] C. Lim, D. Hwang, M. Yazdimamaghani, H. M. Atkins, H. Hyun, Y. Shin, J. D. Ramsey, P. D. Radler, K. R. Mott, C. M. Perou, M. Sokolsky-Papkov, A. V. Kabanov High-Dose Paclitaxel and its Combination with CSF1R Inhibitor in Polymeric Micelles for Chemoimmunotherapy of Triple Negative Breast Cancer *Nano Today* **2023**, *51*, 101884-101898.
[24] L. Hahn, M. M. Lübtow, T. Lorson, F. Schmitt, A. Appelt-Menzel, R. Schobert, R. Luxenhofer Investigating the Influence of Aromatic Moieties on the Formulation of Hydrophobic Natural Products and Drugs in Poly(2-oxazoline)-Based Amphiphiles *Biomacromolecules* **2018**, *19*, 3119-3128.
[25] J. D. Ramsey, I. E. Stewart, E. A. Madden, C. Lim, D. Hwang, M. T. Heise, A. J. Hickey, A. V. Kabanov Nanoformulated Remdesivir with Extremely Low Content of Poly(2-oxazoline)-Based Stabilizer for Aerosol Treatment of COVID-19 *Macromol Biosci* **2022**, *22*, 2200056-2200067.
[26] C. D'Amico, A. L. Ziegler, M. Kemell, G. Molinaro, R. Luxenhofer, H. A. Santos Self-Nanoformulating Poly(2-oxazoline) and Poly(2-oxazine) Copolymers Based Amorphous Solid Dispersions as Microneedle Patch: A Formulation Study *Adv Mater Technol* **2024**, 2400766-2400775.
[27] J. Li, H. Pan, Q. Ye, C. Shi, X. Zhang, W. Pan Carvedilol-loaded polyvinylpyrrolidone electrospun nanofiber film for sublingual delivery *J Drug Deliv Sci Technol* **2020**, *58*, 101726-101732.
[28] S. Mares-Bou, M. A. Serrano, J. A. Gomez-Tejedor Core-Shell Polyvinyl Alcohol (PVA) Base Electrospinning Microfibers for Drug Delivery *Polymers (Basel)* **2023**, *15*, 1554-1573.
[29] H. Lv, D. Tang, Z. Sun, J. Gao, X. Yang, S. Jia, J. Peng Electrospun PCL-based polyurethane/HA microfibers as drug carrier of dexamethasone with enhanced biodegradability and shape memory performances *Colloid Polym Sci* **2019**, *298*, 103-111.
[30] J. Xie, C. H. Wang Electrospun micro- and nanofibers for sustained delivery of paclitaxel to treat C6 glioma in vitro *Pharm Res* **2006**, *23*, 1817-1826.
[31] F. L. Lopez, G. C. Shearman, S. Gaisford, G. R. Williams Amorphous formulations of indomethacin and griseofulvin prepared by electrospinning *Mol Pharm* **2014**, *11*, 4327-4338.
[32] J. Ye, M. Gong, J. Song, S. Chen, Q. Meng, R. Shi, L. Zhang, J. Xue Integrating Inflammation-Responsive Prodrug with Electrospun Nanofibers for Anti-Inflammation Application *Pharmaceutics* **2022**, *14*, 1273-1287.

[33] T. Xu, J. Gu, J. Meng, L. Du, A. Kumar, H. Xu Melt electrowriting reinforced composite membrane for controlled drug release *J Mech Behav Biomed Mater* **2022**, *132*, 105277-105285.
[34] A. Mathew, B. L. Devlin, D. Singh, N. C. Paxton, M. A. Woodruff Improving Infection Resistance in Tissue Engineered Scaffolds for Tensile Applications Using Vancomycin-Embedded Melt Electrowritten Scaffolds *Macromol Mater Eng* **2023**, *308*, 2300168-2300177.
[35] J. Bai, H. Wang, W. Gao, F. Liang, Z. Wang, Y. Zhou, X. Lan, X. Chen, N. Cai, W. Huang, Y. Tang Melt electrohydrodynamic 3D printed poly (epsilon-caprolactone)/polyethylene glycol/roxithromycin scaffold as a potential anti-infective implant in bone repair *Int J Pharm* **2020**, *576*, 118941-118949.
[36] D. A. Miller, J. C. DiNunzio, W. Yang, J. W. McGinity, R. O. Williams, 3rd Enhanced in vivo absorption of itraconazole via stabilization of supersaturation following acidic-to-neutral pH transition *Drug Dev Ind Pharm* **2008**, *34*, 890-902.
[37] E. Immergut, H. Mark, in *Advances in Chemistry, Vol. 48*, ACS, **1965**, pp. 1-26.
[38] C. E. Correa-Soto, Y. Gao, A. S. Indulkar, G. G. Z. Zhang, L. S. Taylor Release Enhancement by Plasticizer Inclusion for Amorphous Solid Dispersions Containing High T(g) Drugs *Pharm Res* **2023**, *40*, 777-790.
[39] F. Hess, T. Kipping, W. Weitschies, J. Krause Understanding the Interaction of Thermal, Rheological, and Mechanical Parameters Critical for the Processability of Polyvinyl Alcohol-Based Systems during Hot Melt Extrusion *Pharmaceutics* **2024**, *16*, 472-492.
[40] K. Wdowiak, L. Tajber, A. Miklaszewski, J. Cielecka-Piontek Sweeteners Show a Plasticizing Effect on PVP K30—A Solution for the Hot-Melt Extrusion of Fixed-Dose Amorphous Curcumin-Hesperetin Solid Dispersions *Pharmaceutics* **2024**, *16*, 659-681.
[41] L. Viidik, J. Vesala, R. Laitinen, O. Korhonen, J. Ketolainen, J. Aruvali, K. Kirsimae, K. Kogermann, J. Heinamaki, I. Laidmae, T. Ervasti Preparation and characterization of hot-melt extruded polycaprolactone-based filaments intended for 3D-printing of tablets *Eur J Pharm Sci* **2021**, *158*, 105619-105627.
[42] K. Biedrzycka, A. Marcinkowska The Use of Hot Melt Extrusion to Prepare a Solid Dispersion of Ibuprofen in a Polymer Matrix *Polymers (Basel)* **2023**, *15*, 2912-2926.
[43] M. Monschke, K. Kayser, K. G. Wagner Processing of Polyvinyl Acetate Phthalate in Hot-Melt Extrusion-Preparation of Amorphous Solid Dispersions *Pharmaceutics* **2020**, *12*, 337-352.
[44] V. R. Kallakunta, S. Sarabu, S. Bandari, A. Batra, V. Bi, T. Durig, M. A. Repka Stable amorphous solid dispersions of fenofibrate using hot melt extrusion technology: Effect of formulation and process parameters for a low glass transition temperature drug *J Drug Deliv Sci Technol* **2020**, *58*, 101395-101404.
[45] A. Chivate, A. Garkal, K. Hariharan, T. Mehta Exploring novel carrier for improving bioavailability of Itraconazole: Solid dispersion through hot-melt extrusion *J Drug Deliv Sci Technol* **2021**, *63*, 102541-102550.
[46] L. Chaunier, L. Viau, X. Falourd, D. Lourdin, E. Leroy A drug delivery system obtained by hot-melt processing of zein plasticized by a pharmaceutically active ionic liquid *J Mater Chem B* **2020**, *8*, 4672-4679.
[47] H. Witte, W. Seeliger Simple synthesis of 2-substituted 2-oxazolines and 5, 6-dihydro-4H-1, 3-oxazines *Angew Chem, Int Ed Engl* **1972**, *11*, 287-288.
[48] F. M. Wunner, O. Bas, N. T. Saidy, P. D. Dalton, E. M. D.-J. Pardo, D. W. Hutmacher Melt electrospinning writing of three-dimensional poly (ε-caprolactone) scaffolds with controllable morphologies for tissue engineering applications *JoVE* **2017**, 56289-56300.
[49] M. M. Bloksma, R. M. Paulus, H. P. van Kuringen, F. van der Woerdt, H. M. Lambermont-Thijs, U. S. Schubert, R. Hoogenboom Thermoresponsive poly(2-oxazine)s *Macromol Rapid Commun* **2012**, *33*, 92-96.

[50] A. G. Tabriz, N. Scoutaris, Y. Gong, H. W. Hui, S. Kumar, D. Douroumis Investigation on hot melt extrusion and prediction on 3D printability of pharmaceutical grade polymers *Int J Pharm* **2021**, *604*, 120755-120765.
[51] S. S. Gupta, A. Meena, T. Parikh, A. T. M. Serajuddin Investigation of thermal and viscoelastic properties of polymers relevant to hot melt extrusion - I: Polyvinylpyrrolidone and related polymers. *J Excipients and Food Chem* **2014**, *5*, 32-45.
[52] A. Meena, T. Parikh, S. S. Gupta, A. T. M. Serajuddin Investigation of thermal and viscoelastic properties of polymers relevant to hot melt extrusion - II: Cellulosic polymers. *J Excipients and Food Chem* **2014**, *5*, 46-55.
[53] G. Hochleitner, J. F. Hümmer, R. Luxenhofer, J. Groll High definition fibrous poly(2-ethyl-2-oxazoline) scaffolds through melt electrospinning writing *Polymer* **2014**, *55*, 5017-5023.
[54] M. L. Williams, R. F. Landel, J. D. Ferry The Temperature Dependence of Relaxation Mechanisms in Amorphous Polymers and Other Glass-forming Liquids *J Am Chem Soc* **2002**, *77*, 3701-3707.
[55] S. M. Krull, H. V. Patel, M. Li, E. Bilgili, R. N. Dave Critical material attributes (CMAs) of strip films loaded with poorly water-soluble drug nanoparticles: I. Impact of plasticizer on film properties and dissolution *Eur J Pharm Sci* **2016**, *92*, 146-155.
[56] P. Jantrawut, T. Chaiwarit, K. Jantanasakulwong, C. H. Brachais, O. Chambin Effect of Plasticizer Type on Tensile Property and In Vitro Indomethacin Release of Thin Films Based on Low-Methoxyl Pectin *Polymers (Basel)* **2017**, *9*, 289-302.